

# High-Resolution Axonal Bundle (Fascicle) Assessment and Triple-Echo Steady-State T<sub>2</sub> Mapping of the Median Nerve at 7 T Preliminary Experience

Georg Riegler, MD,\* Gregor Drlicek,\* Claudia Kronnerwetter,\* Rahel Heule, MSc,† Oliver Bieri, PhD,‡ Gerd Bodner, MD,\* Doris Lieba-Samal, MD,‡ and Siegfried Trattnig, MD\*

**Objectives:** The aims of this preliminary study were to determine the number of axonal bundles (fascicles) in the median nerve,<sup>1</sup> using a high-resolution, proton density (PD)-turbo spin echo (TSE) fat suppression sequence, and to determine normative T<sub>2</sub> values, measured by triple-echo steady state, of the median nerve in healthy volunteers and in patients with idiopathic carpal tunnel syndrome (CTS), at 7 T.<sup>2</sup>

**Materials and Methods:** This prospective study was approved by the local ethics committee and conducted between March 2014 and January 2015. All study participants gave written informed consent. Six healthy volunteers (30 ± 12 years) and 5 patients with CTS (44 ± 16 years) were included. Measurements were performed on both wrists in all volunteers and on the affected wrist in patients (3 right, 2 left). Based on 5-point scales, 2 readers assessed image quality (1, very poor; 5, very good) and the presence of artifacts that might have a possible influence on fascicle determination (1, severe artifacts; 5, no artifacts) and counted the number of fascicles independently on the PD-TSE sequences. Furthermore, T<sub>2</sub> values by region of interest analysis were assessed. Student *t* tests, a hierarchic linear model, and intraclass correlation coefficients (ICCs) were used for statistical analysis.

**Results:** Proton density-TSE image quality and artifacts revealed a median of 5 in healthy volunteers and 4 in patients with CTS for both readers. Fascicle count of the median nerve ranged from 13 to 23 in all subjects, with an ICC of 0.87 (95% confidence interval [CI], 0.67–0.95). T<sub>2</sub> values were significantly higher (*P* = 0.023) in patients (24.27 ± 0.97 milliseconds [95% CI, 22.19–26.38]) compared with healthy volunteers (21.01 ± 0.65 milliseconds [95% CI, 19.61–22.41]). The ICC for all T<sub>2</sub> values was 0.97 (95% CI, 0.96–0.98).

**Conclusions:** This study shows the possibility of fascicle determination of the median nerve in healthy volunteers and patients with CTS (although probably less accurately) with high-resolution 7 T magnetic resonance imaging, as well as significantly higher T<sub>2</sub> values in patients with CTS, which seems to be associated with pathophysiological nerve changes.

**Key Words:** median nerve, magnetic resonance imaging, biochemical marker, carpal tunnel syndrome, peripheral nerve injury, entrapment neuropathies

(*Invest Radiol* 2016;51: 529–535)

Peripheral neuropathy is a common clinical problem and includes compression syndromes, nerve trauma, inflammation, or tumors. It is estimated that approximately 5% of the population has some form of peripheral neuropathy.<sup>1,2</sup>

Recently, imaging of the peripheral nerves has improved dramatically due to rapid improvements in field strength, coil technology, and sequences, and this will likely increase its impact on diagnosis.

Magnetic resonance (MR) neurography at current clinical field strengths (eg, 1.5 T or 3 T) has shown excellent anatomical capabilities.<sup>3</sup> However, the full identification of the ultrastructural components of peripheral nerves is challenging and not possible in all cases.

Ultrahigh-field (UHF) strength in combination with a recently developed 12-channel wrist coil<sup>4</sup> offers unique possibilities to overcome some limitations in MR neurography. Thus, visualization of the level of the axonal bundle (fascicle) seems to be feasible due to the high signal-to-noise ratio at 7 T.<sup>4</sup> To date, only *ex vivo* studies<sup>5,6</sup> and a few *in vivo* case reports<sup>7,8</sup> have revealed neuronal constituents at this level.

The depiction of individual fascicles (ranging from 12 to 27 in histological sections<sup>9</sup>) may help to distinguish between injuries that require surgery early in the postoperative phase.<sup>10,11</sup> This may enable the surgeon to align fascicles in the correct orientation to match transplants and, thus, reduce postoperative morbidity,<sup>12</sup> or could enhance diagnostic performance for selective fascicular involvement in focal nerve lesions.<sup>13</sup>

Furthermore, in addition to diffusion tensor imaging<sup>14,15</sup> and a few reports in the literature about T<sub>1</sub> and T<sub>2</sub> tissue characterization and magnetization transfer,<sup>16–18</sup> quantitative tissue characterization, which reflects the properties of biological tissues at a submicroscopic level, has, to date, played a minor role in nerve tissue evaluation. T<sub>2</sub> mapping is sensitive to the water microenvironment that reflects the biological properties of nerve tissue. It provides quantification of the increased T<sub>2</sub> signal in pathological nerves and may, therefore, offer potential in diagnosis and disease control of nerve entrapment syndromes, inflammatory nerve pathologies, nerve regeneration, or follow-up.

A recently introduced 3-dimensional (3D) triple-echo steady-state (TESS) relaxometry technique has been proposed for rapid T<sub>1</sub> and T<sub>2</sub> quantification.<sup>19</sup> Compared with the previously used multiecho spin echo (SE) sequences or conventional steady-state free precession sequences,<sup>20–22</sup> TESS provides multiple benefits, such as the rapid measurement of T<sub>1</sub> and T<sub>2</sub> rapidly in 1 single scan<sup>19</sup> and the fact that it is insensitive to B<sub>1</sub> inhomogeneities.<sup>23</sup>

The investigation of the human median nerve is of clinical interest because it is affected by the most common entrapment neuropathy in the human body—carpal tunnel syndrome (CTS),<sup>24,25</sup> with its relatively large size (~2–3 mm cross section) and superficial location at the wrist.

Therefore, the aims of this preliminary study were to determine the number of axonal bundles (fascicles) in the median nerve, using a high-resolution proton density (PD)-turbo SE (TSE) fat suppression sequence,<sup>1</sup> and to determine normative T<sub>2</sub> values, measured by TESS, of the median nerve in healthy volunteers and in patients with idiopathic CTS at 7 T.<sup>2</sup>

## MATERIALS AND METHODS

### Study Participants

This prospective study was approved by the local ethics committee of the Medical University of Vienna (EC-number 1865/2013) and was conducted between March 2014 and January 2015. All study participants gave written informed consent. Six healthy volunteers (3 female, 3 male; mean age, 30 years; age range, 22–42 years) and 5 patients with CTS (5 women; mean age, 44 years; age range, 28–54 years) were

Received for publication October 29, 2015; and accepted for publication, after revision, January 9, 2016.

From the \*MR Centre of Excellence, Department of Biomedical Imaging and Image-Guided Therapy, Medical University of Vienna, Vienna, Austria; †Division of Radiological Physics, Department of Radiology, University of Basel Hospital, Basel, Switzerland; and ‡Department of Neurology, Medical University of Vienna, Vienna, Austria.

Conflicts of interest and sources of funding: none declared.

Correspondence to: Georg Riegler, MD, MR Centre of Excellence, Department of Biomedical Imaging and Image-Guided Therapy, Medical University of Vienna, Lazarettgasse 14, 1090 Vienna, Austria. E-mail: georg.riegler@meduniwien.ac.at

Copyright © 2016 Wolters Kluwer Health, Inc. All rights reserved.

ISSN: 0020-9996/16/5108–0529

DOI: 10.1097/RLI.0000000000000265

included in the study. Measurements were performed on the left and right wrist in all volunteers and on the affected wrist in patients (3 right, 2 left).

The healthy volunteers scanned were recruited from an established volunteer pool of the MR Centre of Excellence at the Medical University of Vienna.

Patients were recruited and examined in the outpatient clinic of Neurology at the Medical University of Vienna by a neurologist (D.L.S.) with special knowledge in electrodiagnostic testing. Inclusion criteria for patients were an age of at least 18 years and a diagnosis of CTS based on typical clinical history, symptoms, and signs (eg, numbness, [nightly] tingling, burning, or pain in at least 2 of the first, second, or third digits, palm pain, wrist pain, atrophy of the thenar muscle, positive Phalen or Hofmann-Tinel sign) as well as compatible electrodiagnostic findings.<sup>26,27</sup>

Exclusion criteria for all study participants were contraindications for MR imaging, pregnancy, central nervous system disorders, previous wrist injury or surgery, and endocrine, metabolic, neuromuscular, or relevant musculoskeletal disorders (such as rheumatoid arthritis, osteoarthritis, osteoporosis, or any form of myositis).

## MR Examination

All participants underwent MR examinations on a 7 T whole-body investigational MR unit (Siemens, Erlangen, Germany) with a dedicated transmit/receive 12-channel wrist coil (RAPID Biomedical GmbH, Rimpfing, Germany).<sup>4</sup> The transmit coil consisted of a completely shielded 24-leg bandpass birdcage with an inner diameter of 180 mm and a length of 210 mm. The birdcage was quadrature-driven using a quadrature hybrid rather than a transmit-receive switch. The receive array coil elements were distributed over a curved surface plate of 12 cm in length and 13 cm in breadth. Considering the depth of the region of interest (ROI) and the possibilities of parallel acquisitions, 12 elements of  $35 \times 35 \text{ mm}^2$  in size were distributed. Neighboring elements were overlapped to minimize coupling between them, whereas the coupling between “next-nearest” elements was reduced by connecting the elements to low-impedance preamplifiers. The participants were placed in a prone position, with the arms elevated over the head (Superman position). Morphological imaging sequences and biochemical  $T_2$  mapping MR imaging methods were used.

Coronal, sagittal, and axial 2-dimensional FLASH gradient echo sequences with fat suppression (repetition time (milliseconds)/echo time (milliseconds), 50/5.6; flip angle, 7 degrees; field of view,  $120 \times 120 \text{ mm}^2$ ; matrix size,  $444 \times 444$ ; voxel size,  $0.3 \times 0.3 \times 1 \text{ mm}^3$ ; number of slices, 3; acquisition time, 25 seconds) were acquired to identify anatomical structures and, thus, precisely define the course of the median nerve in the region of the wrist. Accordingly, the nerve was tangentially marked in its length in the sagittal and coronal planes and orthogonally in the axial plane.

The determined parameters, considering the nerve's course through the wrist, adapted the orientation of slicing in all 3 axes for the following axial PD-TSE sequence with fat suppression (repetition time milliseconds/echo time milliseconds, 4000/ 31; turbo factor, 6; flip angle, 180 degrees; field of view,  $120 \times 72 \text{ mm}^2$ ; matrix size,  $1024 \times 612$ ; voxel size,  $0.1 \times 0.1 \times 2.5 \text{ mm}^3$ ; number of slices, 10; acquisition time, 5 minutes 34 seconds) to allow an as much as possible orthogonal sectioning of the nerve in the axial plane for optimal countability of fascicles.

For biochemical assessment, an axial 3D TESS was used to generate  $T_2$  images and calculate  $T_2$  relaxation times of the median nerve. To enable short TR and, thus, mitigate possible susceptibility effects, the 3 steady-state free precession signal amplitudes were acquired within 3 consecutive TR intervals (each within 1 at the same echo time).<sup>19</sup> TESS imaging included the following parameters: repetition time (milliseconds)/echo time (milliseconds), 6.37/3.16; flip angle, 15 degrees; field of view,  $160 \times 160 \text{ mm}^2$ ; matrix size,  $320 \times 320 \times 18$ ; voxel

size,  $0.5 \times 0.5 \times 2 \text{ mm}^3$ ; number of slices, 18; acquisition time, 5 minutes 44 seconds.

## Data Processing Qualitative Diagnostic Image Quality Scores and Fascicle Count

Images were analyzed with Syngo MR VB 17 software (Siemens Healthcare, Erlangen, Germany). A board-certified radiologist with 22 years of experience in musculoskeletal imaging (S.T., reader 1) and a resident in radiology with 4 years of experience in musculoskeletal imaging (G.R., reader 2) interpreted all MR studies independently and were blinded to each other's results.

First, all PD-TSE images were assessed for image quality (eg, resolution, anatomical structure details) and the presence of artifacts that might have a possible influence on fascicle determination (eg, motion artifacts, ghosting artifacts). The overall image quality was rated using a 5-point scale as very good (5), good (4), average (3), poor (2), or very poor (1). The presence of artifacts was scored on a 5-point scale: a score of 1 indicated severe artifacts (nondiagnostic); a score of 2 indicated severe artifacts, some fascicles visible (nondiagnostic), a score of 3 indicated moderate artifacts (limited diagnosis); a score of 4 indicated mild artifacts (little or no effect on diagnosis); and a score of 5 indicated no artifacts.

Second, the morphological appearance of 5 different nerve/fascicle characteristics was assessed on 3-point scales as follows: nerve swelling (1, prominent; 2, present; 3, absent); fascicle swelling (1, prominent; 2, present; 3, absent); epineurium of the median nerve (defined as well-defined low signal intensity ring corresponding to the outer margin of the nerve) distinguishable (1, not distinguishable; 2, partly distinguishable; 3, distinguishable); subfascicular endoneurium (interlacing low signal intensity tissue within the fascicles) detectable (1, not detectable; 2, partly detectable; 3, detectable); and fascicle delineation (1, no; 2, almost; 3, clear).

Third, the readers counted the number of fascicles.

## $T_2$ Assessment

Reader 1 and reader 2 assessed quantitative  $T_2$  images. Both worked independently and were blinded to each other's results. In case of unclear findings (eg, borders of the nerve not distinguishable from surrounding tissue), both readers arrived at a consensus finding.  $T_2$  values were calculated from raw  $T_2$  images using Syngo MR VB 17 software. Every slice was evaluated separately. In the tab “Color lookup table,” the “Rainbow 16 Bit” was chosen. The morphological PD-TSE slices that corresponded most closely to the  $T_2$  map served as an anatomical reference. With respect to the cross-section of the nerve in the most closely corresponding morphological PD-TSE image, a free-hand ROI was drawn carefully onto the  $T_2$  maps. Consequently, the borders of the nerve were defined to determine the voxels that should have been included in the automatic  $T_2$  calculation (Fig. 1). By adjusting the cross-sectional area of the  $T_2$  map to the cross-sectional area determined in the morphological image, the voxels that best fit the shape of the nerve were included in the  $T_2$  calculation. Thus,  $T_2$  values reflected not only the proper nerve fibers and fascicles, but also the nerve in its entire composition, most importantly including the characteristic connective tissue layers, such as the endoneurium, perineurium, and epineurium. For further analysis, 2 different anatomical regions were defined. One region was outside the carpal tunnel at the level of the radioulnar joint, and one was inside the tunnel at the level of the pisiform bone. The TESS sequence resulted in 18 slices per wrist. Two slices at the proximal and distal end of the imaged nerve were excluded for evaluation to avoid measurement errors due to possible artifacts. In total, 14 slices were analyzed, resulting in a total of 238 possible  $T_2$  maps for healthy volunteers (168  $T_2$  maps) and patients (70  $T_2$  maps). In total, of the 238 possible ROIs, 26 (20 in healthy volunteers; 6 in

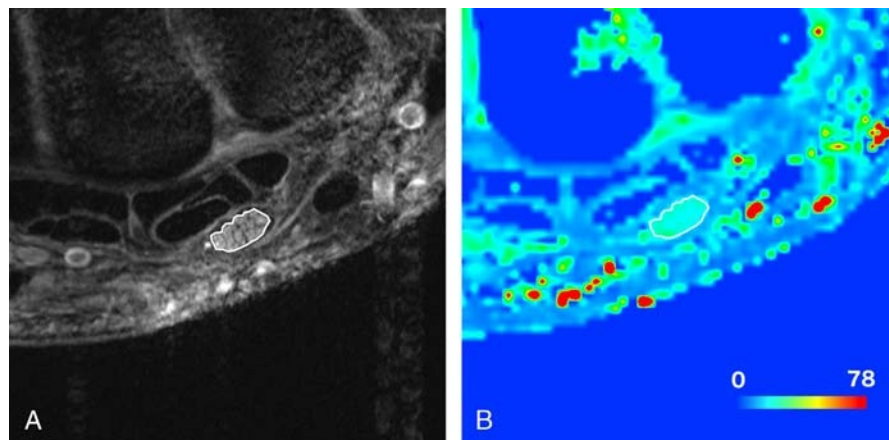


**FIGURE 1.** Screenshot series shows a T<sub>2</sub> map obtained by the TESS sequence (B) and the PD-TSE image (A) that corresponded most closely for anatomic correlation. Images show ROI placement on the PD-TSE image for measurement of the cross-sectional area of the median nerve and on the T<sub>2</sub> map to obtain T<sub>2</sub> values. Figure 1 can be viewed online in color at [www.investigativeradiology.com](http://www.investigativeradiology.com).

patients) were not evaluable because the nerve was not clearly distinguishable from the surrounding tissue. Therefore, 148 T<sub>2</sub> maps (88%) in healthy volunteers and 64 (91%) in patients were useful for analysis. T<sub>2</sub> values were assessed on all 168 T<sub>2</sub> maps.

**Statistical Analysis**

A statistician using IBM SPSS Statistics for Windows Version 22.0.0.2 (IBM, Armonk, NY) performed all statistical computations. Metric data, such as T<sub>2</sub> values or fascicle counts, are presented as mean ± standard deviation. For qualitative diagnostic image quality scores, median, minimum, and maximum were used. Percentage of agreement and a κ value were calculated to assess rater agreement and interobserver variability for qualitative diagnostic image quality scores. A κ value of 0.81 to 1.00 indicated excellent agreement; a κ value of 0.61 to 0.80, substantial agreement; a κ value of 0.41 to 0.60, moderate agreement; a κ value of 0.21 to 0.40, fair agreement; and a

κ value of 0.00 to 0.20, slight agreement. Fascicle counts are presented as a range (minimum to maximum). A statistical power estimation for T<sub>2</sub> values was performed. To take multiple measures into account, a hierarchical linear model was used to compare T<sub>2</sub> values between patients and healthy volunteers over the whole nerve and in 2 anatomic regions (radioulnar joint and pisiform bone). Calculations were performed with 3 different types of covariance matrices: (a) assuming compound symmetry, (b) unstructured, and (c) AR1. As the unstructured model showed the best model fit (using Bayesian Information Criterion), these results are presented. To compare differences between the left and right median nerve in healthy volunteers, a paired Student *t* test was performed. Two-way mixed intraclass correlation coefficients (ICCs) and their 95% confidence intervals (CIs) were used as an index of rater agreement. Intraclass correlation coefficients were interpreted according to the criteria of Landis and Koch<sup>28</sup>: an ICC of 0.01 to 0.20 indicated slight agreement; an ICC of 0.21 to 0.40, fair agreement; an

**TABLE 1.** Qualitative Diagnostic Image Quality Scores of PD TSE Images

	Healthy Volunteers						κ	Agreement
	Reader 1			Reader 2				
	Median	Minimum	Maximum	Median	Minimum	Maximum		
Image quality	5	4	5	5	3	5	0.33	66.7%
Artifacts	5	3	5	5	4	5	0.62	83.3%
Nerve swelling	3	2	3	3	2	3	1.00	100.0%
Fascicle swelling	3	2	3	3	2	3	1.00	100.0%
Epineurium	3	2	3	3	2	3	0.75	91.7%
Subfascicular endoneurium	3	1	3	3	2	3	0.37	75.0%
Fascicle delineation	3	2	3	3	2	3	1.00	100%
	Patient						κ	Agreement
	Reader 1			Reader 2				
	Median	Minimum	Maximum	Median	Minimum	Maximum		
Image quality	4	4	5	4	3	5	0.44	60.0%
Artifacts	4	3	5	4	3	5	1.00	100.0%
Nerve swelling	1	1	2	1	1	2	1.00	100.0%
Fascicle swelling	1	1	2	1	1	2	0.55	80.0%
Epineurium	2	1	3	2	1	3	0.69	80.0%
Subfascicular endoneurium	2	1	2	2	1	2	0.55	80.0%
Fascicle delineation	2	2	2	2	2	2	1.00	100.0%

**TABLE 2.** Fascicle Count for Reader 1 and Reader 2 in Healthy Volunteers and Patients With CTS

Healthy Volunteers Number	Reader 1	Reader 2
1	16	17
2	17	19
3	20	19
4	19	20
5	15	17
6	14	15
7	21	22
8	21	23
9	23	22
10	20	19
11	18	17
12	21	18
Patients Number	Reader 1	Reader 2
1	16	15
2	13	13
3	17	17
4	16	15
5	18	16

CTS indicates carpal tunnel syndrome.

ICC of 0.41 to 0.60, moderate agreement; an ICC of 0.61 to 0.80, substantial agreement; and an ICC of 0.81 to 1.00, almost perfect agreement. A *P* value equal to or below 5% was considered to indicate significant results.

## RESULTS

### Qualitative Diagnostic Image Quality Scores and Fascicle Count

Figure 1 shows a table of all qualitative diagnostic image quality scores of the high-resolution morphological PD-TSE

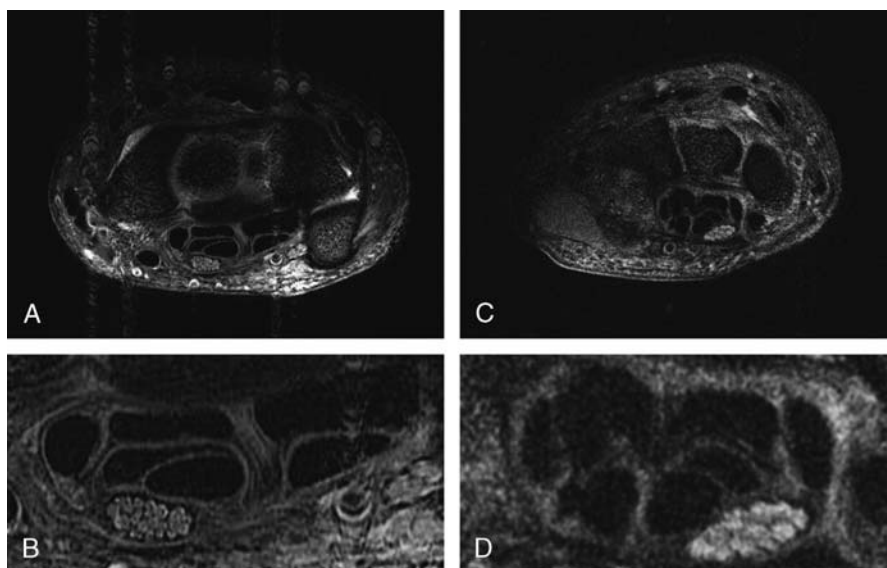
images, the  $\kappa$  values, and percentage of agreement (Table 1). Comprehensive results of the fascicle counts are presented in Table 2. The fascicle count of the median nerve ranged from 13 to 23 in all subjects. The ICC for fascicle counts was 0.87 (95% CI, 0.67–0.95) for all subjects, indicating an almost perfect agreement. Visualized examples of evaluated slices in healthy volunteers and in patients with CTS are shown in Figure 2.

### T<sub>2</sub> Assessment

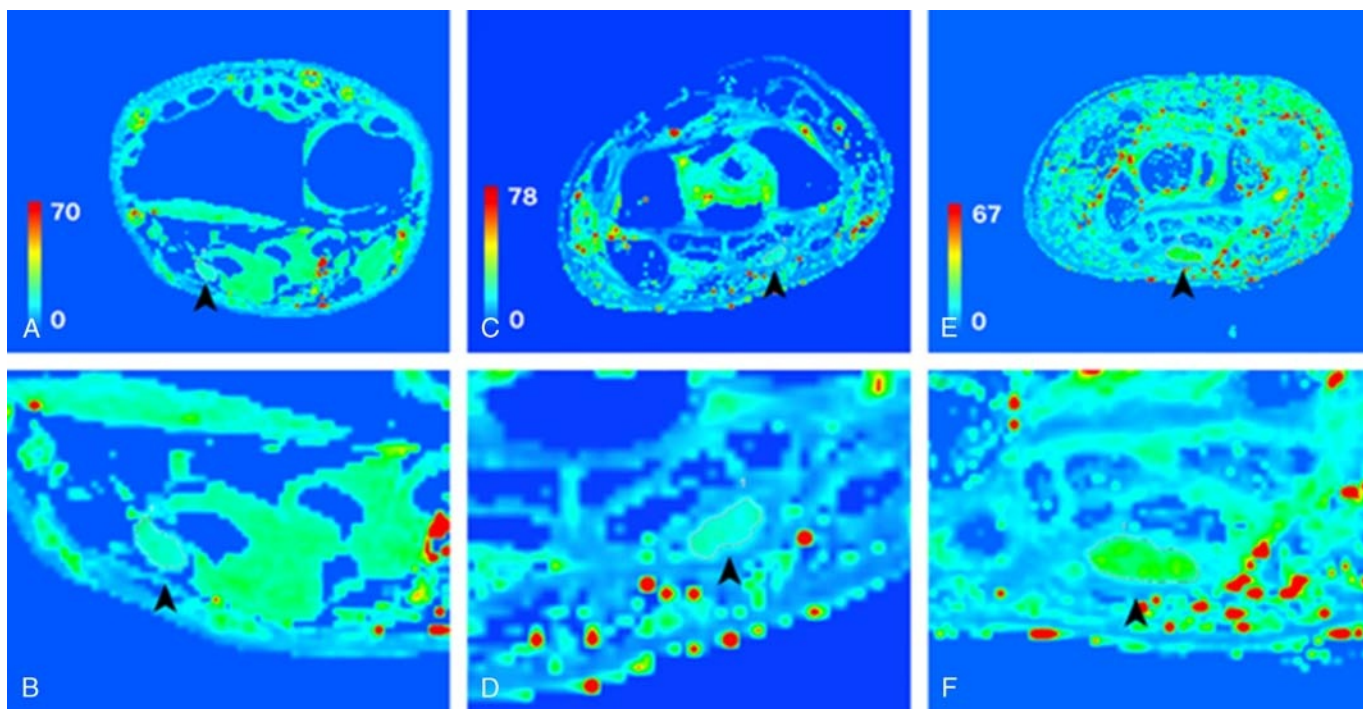
Statistical power for T<sub>2</sub> values was 90%. T<sub>2</sub> values of the median nerve at the level of the wrist resulted in a mean of 21.01 ± 0.65 milliseconds (95% CI, 19.61–22.41) in healthy volunteers. The right median nerve revealed a mean T<sub>2</sub> value of 20.83 ± 1.78 milliseconds (95% CI, 18.62–23.04) and the left median nerve a mean T<sub>2</sub> value of 21.17 ± 2.14 milliseconds (95% CI, 18.52–23.82). There were no statistically significant differences between the right and left median nerve (*P* = 0.655). T<sub>2</sub> values of the median nerve in patients with CTS were 24.27 ± 0.97 milliseconds (95% CI, 22.19–26.38). T<sub>2</sub> values in patients were significantly higher compared with those in healthy volunteers (*P* = 0.023). Figure 3 shows an example of a T<sub>2</sub> map of a healthy volunteer and a patient with CTS.

Figure 4 shows box plots of T<sub>2</sub> values at 2 different anatomical locations (radioulnar joint and pisiform bone). T<sub>2</sub> values at the level of the radioulnar joint were 19.16 ± 0.57 milliseconds (95% CI, 17.94–20.37) in healthy volunteers and 22.36 ± 0.83 milliseconds (95% CI, 20.54–24.19) in patients, indicating statistically significantly higher values in patients with CTS (*P* = 0.008) compared with healthy volunteers. T<sub>2</sub> values at the level of the pisiform bone were 20.74 ± 1.04 milliseconds (95% CI, 18.48–22.99) in healthy volunteers and 28.14 ± 1.73 milliseconds (95% CI, 24.39–31.89) in patients, indicating statistically significantly higher values in patients with CTS (*P* = 0.003) compared with healthy volunteers. Notably, the increase of T<sub>2</sub> values in patients with CTS compared with that of healthy volunteers was even more pronounced at the level of the pisiform bone (within the carpal tunnel) in contrast to those at the level of the radioulnar joint.

The ICC for T<sub>2</sub> values of the median nerve over its entire course was 0.97 (95% CI, 0.96–0.98) in all study participants, 0.95 (95% CI, 0.93–0.96) for healthy volunteers, and 0.97 (95% CI,



**FIGURE 2.** Axial PD-TSE images of the wrist (A and C) and a close-up of the carpal tunnel region (B and D) at 7 T. Right wrist of a 23-year-old healthy female patient (fascicle count: reader 1, 23; reader 2, 22). Left wrist of a 28-year-old female patient with CTS (fascicle count: reader 1, 13; reader 2, 13). Note the swollen fascicles and the diminished interfascicular tissue in the patient with CTS.



**FIGURE 3.** Axial T<sub>2</sub> maps at the level of radioulnar joint (A and B) and the wrist in the carpal tunnel region (C–F) at 7 T acquired with TESS. Freehand ROI placed by reader 1. Left wrist of a 24-year-old female healthy volunteer with a T<sub>2</sub> value of 18.60 milliseconds (A and B). Left wrist (C and D) of a 24-year-old female healthy volunteer with a T<sub>2</sub> value of 20.00 milliseconds. Left wrist (E and F) of a 23-year-old female patient with CTS, with a T<sub>2</sub> value of 33.40 milliseconds. Color bars indicate the range of T<sub>2</sub> values in the presented images. Arrowheads point at the median nerve. Figure 3 can be viewed online in color at [www.investigativeradiology.com](http://www.investigativeradiology.com).

0.95–0.99) for patients with CTS, indicating an almost perfect agreement in all measurements.

## DISCUSSION

Our study demonstrated the feasibility of the visualization and quantification of the ultrastructural components of the median nerve at the axonal bundle level, and the ability to perform rapid quantification of T<sub>2</sub> relaxation times of the median nerve at the level of the wrist at 7 T, in healthy volunteers and in patients with CTS. Fascicle count, in these subjects, revealed an ICC of 0.87, indicating an almost perfect agreement between raters that enabled a quantification with only slight imprecision. In healthy volunteers, the fascicle count of our study revealed results comparable to those of the anatomical standard of reference used,<sup>9</sup> whereas in patients with CTS, the fascicle count slightly diminished. Notably, overall scan time was approximately 12 minutes, representing a clinically acceptable measurement time for morphological and biochemical evaluation of the median nerve tissue at the wrist.

Interestingly, the median nerve has, thus far, not been a primary focus of interest for in vivo imaging at UHF strengths, either in healthy volunteers or in patients with CTS. A few studies, with high-resolution imaging of the wrist as their study goal, could identify some individual fascicles as small foci of intermediate signal intensity at UHF strengths up to 8 T.<sup>7,8</sup> The potential of multichannel phased array coils to further improve image quality in images of the wrist was shown by Chang and colleagues.<sup>7</sup> Some fascicles were distinguishable, but because of the fact that this protocol was not exclusively optimized for the depiction of the median nerve, no further statement with regard to the fascicle number was possible.

Bilgen et al<sup>5</sup> and Heddings et al<sup>6</sup> in ex vivo studies at 9.4 T demonstrated excellent delineation of nerve tissue at UHF strength. In both studies, it was possible to distinguish fascicles, the interfascicular epineurium, the perineurium, and even intrafascicular septations. It is of further note that the second echo in the multislice dual-echo scan, having a longer TE and obtaining T<sub>2</sub> contrast, provided some benefits

compared with the shorter TE PD-weighted image. Longer TE obviously enhances the perineurium signal circumferentially surrounding the fascicle and improves the image contrast within the fascicles. In our study, we used a TE of 31 milliseconds to accommodate this knowledge and to produce an optimal signal for fascicle depiction.

In contrast to these cadaver studies, our in vivo study showed some signal characteristics different than those of the median nerve. The whole fascicle revealed a brighter signal; consequently, the bundles

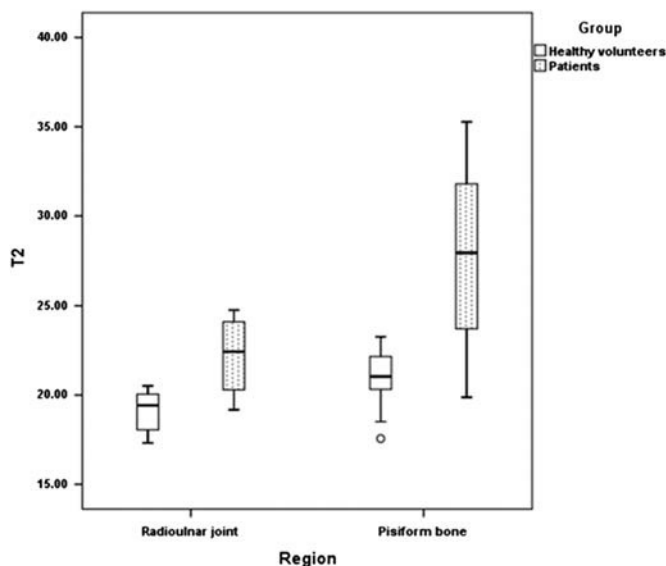


**FIGURE 4.** Box plots of regional T<sub>2</sub> differences in healthy volunteers and patients with CTS.

of nerve fibers within the endoneurium were not as clearly visible as in cadaver studies. Furthermore, the perineurium surrounding each fascicle did not show as bright a signal as in the aforementioned *ex vivo* studies, but was clearly detectable in most cases. We think that this difference is mainly explainable by the different physiological conditions in *vivo* and *ex vivo*, such as blood supply and the different water content of the median nerve, so the direct comparison of data is limited by these factors. Furthermore, it has to be pointed out that, in our study in patients with CTS, the number of fascicles decreased, indicating that some fascicles were no longer detectable, mainly because of the swelling of the whole nerve. Nevertheless, we think that the high-resolution obtained in this study may enhance the noninvasive assessment of acute peripheral nerve injuries,<sup>10,11</sup> and therefore, enhance the outcome of a potential surgical procedure and decrease perisurgical and postsurgical complications, such as iatrogenic nerve tissue trauma, neuroma in continuity formation, or intraneural fibrosis.<sup>29</sup> Nevertheless, further studies to enhance MR imaging techniques and coils are needed to reliably answer these questions.

Moreover, visualization of individual fascicles may enhance diagnostic capabilities where certain fascicles of a nerve and not the whole nerve are affected (eg, the anterior interosseous nerve syndrome, neuritis, or tumor infiltration of individual fascicles) or may further improve surgical planning for difficult anatomical conditions (eg, tumor excision with nerve/fascicle involvement).<sup>12,13</sup>

This is the first study to assess the feasibility of investigating the median nerve with  $T_2$  mapping using a 3D TESS at 7 T. Furthermore, the quantification of  $T_2$  relaxation times with 3D TESS, thus far performed only in cartilage,<sup>19</sup> was first applied to peripheral nerve structures. High-resolution morphological imaging and  $T_2$  mapping of the median nerve were performed with a dedicated 12-channel receive/transmit array coil that facilitated signal acquisition with high signal to noise ratio at 7 T. The highest number of channels when using multichannel array coils thus far was a 4-channel transmit/8-channel receive coil.<sup>7,30</sup>

Assessment of  $T_2$  time is a quantitative method by which to characterize tissue properties, especially the interaction of water protons on a cellular level.<sup>23</sup> To the best of our knowledge, only 2 studies of median nerve  $T_2$  mapping at 3 T<sup>17</sup> and 7 T<sup>18</sup> exist. Moreover, data about  $T_2$  values in patients with CTS are not available as yet.

Mean values of  $T_2$  relaxation times, acquired with TESS (21.01 ± 0.65 milliseconds) in healthy volunteers, were in good agreement with those acquired with the reference single-echo SE approach at 7 T (18.3 ± 1.9 milliseconds).<sup>18</sup> Nevertheless, a valid comparison between both techniques requires measurements on the same patients, which was not the primary goal of this study.

The ultimate goal of establishing normative  $T_2$  values is to have a reference standard and to compare normative and abnormal values. In our study, we found a significant increase ( $P = 0.023$ ) of mean  $T_2$  values for nerves affected by CTS compared with healthy nerves. Although our study samples were not age matched, this increase was depicted in our younger patients as well as our older patients, and is mainly influenced by the severity of CTS and not by the age of the patient. For example, the youngest person with CTS in our study (28 years) had a  $T_2$  value of 26.76 milliseconds, and the oldest (54 years) had 26.52 milliseconds. In most cases, the compression of nerves occurs gradually over time, as a result of increased pressure at sites of anatomic narrowing through which nerves pass. Chronic nerve compression, to a certain degree, does not damage the axon itself, but it is a process of demyelination followed by remyelination of axons if regeneration occurs.<sup>31–33</sup> Webb and colleagues<sup>34</sup> demonstrated that this process is detectable with multicomponent  $T_2$  mapping in crushed sciatic nerves in male Lewis rats, which was also confirmed by histomorphometric findings. Those authors found a clearly marked primary decrease of the short  $T_2$  component and an increase of the intermediate and long  $T_2$  component (the sciatic nerve has 3  $T_2$  relaxation time components) in cases of demyelination, which was followed by the inverse behavior

in cases of remyelination. The  $T_2$  relaxation times of the median nerve have a bimodal signal behavior, as shown by the multiecho SE technique at 3 T with a short  $T_2$  component (26 ± 2 milliseconds), accounting for 80% of the signal intensity, and a smaller long  $T_2$  component (96 ± 3 milliseconds) that accounts for 20% of the signal intensity.<sup>18</sup> The authors stated that the long  $T_2$  value is close to the  $T_2$  of white matter at 3 T (80 milliseconds); thus, it may originate from the intra-axonal water protons of the median nerve. The short component likely derived from spatial compartmentalization of water into myelin and connective tissue because both are characterized by short  $T_2$  values (30–36 milliseconds). Considering the pathophysiology of chronic nerve compression and multicomponent  $T_2$  mapping of median nerve tissue, we hypothesize that, in cases of CTS, the elongation of  $T_2$  relaxation is mainly influenced by the increase of interaxonal and axonal water, and the decreased amount of myelin. This is of particular interest in differentiating between pathologies that have the potential to spontaneously regenerate and nerves that do not, and therefore, require further therapy. Triple-echo steady-state measures the results of both  $T_2$  components in median nerve tissue but does not distinguish between them. However, we think it could be possible to indirectly observe the pathophysiology of CTS with TESS by measuring the resulting  $T_2$ . To address these questions, future studies need to focus on assessing normative and pathological nerve  $T_2$  values, to extract multiple relaxation components associated with the microscopic compartmentalization of water in tissue that might reflect important structural properties of nerves,<sup>35,36</sup> and to match these findings with TESS. If possible, TESS could be a key player in introducing time-efficient  $T_2$  mapping of the median nerve into routine clinical protocols. Triple-echo steady-state was found to be a rapid and precise sequence with which to measure  $T_2$  relaxation times, as it is insensitive to  $B_0$  inhomogeneities and was not affected by either  $B_1$  field errors or by a dependency on  $T_1$  relaxation times. The advantage of the TESS sequence could be seen in the short acquisition time and the possibility to further obtain  $T_1$  relaxation times.<sup>37</sup>

The main limitation of this study is that only a relatively small number of patients were investigated. Further studies will be required to address this issue, as well as the reproducibility over time. Nevertheless, the results obtained in the current study are already statistically significant and may serve as baseline values in healthy volunteers and patients with CTS at 7 T.

In conclusion, this study shows the possibility of fascicle determination of the median nerve in healthy volunteers and patients with CTS (although probably less accurately) with high-resolution 7 T MR imaging, as well as significantly higher  $T_2$  values in patients with CTS, which seem to be associated with pathophysiological nerve changes.

## ACKNOWLEDGMENTS

The authors thank Mary McAllister for her comments on the manuscript and Michael Weber for statistical analysis.

## REFERENCES

1. England JD, Asbury AK. Peripheral neuropathy. *Lancet*. 2004;363:2151–2161.
2. Martyn CN, Hughes RA. Epidemiology of peripheral neuropathy. *J Neurol Neurosurg Psychiatry*. 1997;62(4):310–318.
3. Chhabra A, Zhao L, Carrino JA, et al. MR neurography: advances. *Radiol Res Pract*. 2013;2013:809568.
4. Raghuraman S, Mueller MF, Zbyn S, et al. 12-channel receive array with a volume transmit coil for hand/wrist imaging at 7 T. *J Magn Reson Imaging*. 2013;38:238–244.
5. Bilgen M, Heddings A, Al-Hafez B, et al. Microneurography of human median nerve. *J Magn Reson Imaging*. 2005;21:826–830.
6. Heddings A, Bilgen M, Nudo R, et al. High-resolution magnetic resonance imaging of the human median nerve. *Neurorehabil Neural Repair*. 2004;18:80–87.

7. Chang G, Friedrich KM, Wang L, et al. MRI of the wrist at 7 tesla using an eight-channel array coil combined with parallel imaging: preliminary results. *J Magn Reson Imaging*. 2010;31:740–746.
8. Farooki S, Ashman CJ, Yu JS, et al. In vivo high-resolution MR imaging of the carpal tunnel at 8.0 tesla. *Skeletal Radiol*. 2002;31:445–450.
9. Ikeda K, Houghton VM, Ho KC, et al. Correlative MR-anatomic study of the median nerve. *AJR Am J Roentgenol*. 1996;167:1233–1236.
10. Chhabra A, Ahlawat S, Belzberg A, et al. Peripheral nerve injury grading simplified on MR neurography: as referenced to Seddon and Sunderland classifications. *Indian J Radiol Imaging*. 2014;24:217–224.
11. Sunderland S. The anatomy and physiology of nerve injury. *Muscle Nerve*. 1990;13:771–784.
12. Pabari A, Yang SY, Seifalian AM, et al. Modern surgical management of peripheral nerve gap. *J Plast Reconstr Aesthet Surg*. 2010;63:1941–1948.
13. Stewart JD. Peripheral nerve fascicles: anatomy and clinical relevance. *Muscle Nerve*. 2003;28:525–541.
14. Breckwoldt MO, Stock C, Xia A, et al. Diffusion tensor imaging adds diagnostic accuracy in magnetic resonance neurography. *Invest Radiol*. 2015;50:498–504.
15. Guggenberger R, Eppenberger P, Markovic D, et al. MR neurography of the median nerve at 3.0 T: optimization of diffusion tensor imaging and fiber tractography. *Eur J Radiol*. 2012;81:e775–e782.
16. Gambarota G, Krueger G, Theumann N, et al. Magnetic resonance imaging of peripheral nerves: differences in magnetization transfer. *Muscle Nerve*. 2012;45:13–17.
17. Gambarota G, Mekele R, Mlynarik V, et al. NMR properties of human median nerve at 3 T: proton density, T1, T2, and magnetization transfer. *J Magn Reson Imaging*. 2009;29:982–986.
18. Gambarota G, Veltien A, Klomp D, et al. Magnetic resonance imaging and T2 relaxometry of human median nerve at 7 Tesla. *Muscle Nerve*. 2007;36:368–373.
19. Heule R, Ganter C, Bieri O. Triple echo steady-state (TESS) relaxometry. *Magn Reson Med*. 2014;71:230–237.
20. Bieri O, Scheffler K, Welsch GH, et al. Quantitative mapping of T2 using partial spoiling. *Magn Reson Med*. 2011;66:410–418.
21. Welsch GH, Scheffler K, Mamisch TC, et al. Rapid estimation of cartilage T2 based on double echo at steady state (DESS) with 3 Tesla. *Magn Reson Med*. 2009;62:544–549.
22. Zeineh MM, Parekh MB, Zaharchuk G, et al. Ultrahigh-resolution imaging of the human brain with phase-cycled balanced steady-state free precession at 7 T. *Invest Radiol*. 2014;49:278–289.
23. Heule R, Ganter C, Bieri O. Rapid estimation of cartilage T with reduced T sensitivity using double echo steady state imaging. *Magn Reson Med*. 2014;71:1137–1143.
24. Gelberman RH, Rydevik BL, Pess GM, et al. Carpal tunnel syndrome. A scientific basis for clinical care. *Orthop Clin North Am*. 1988;19:115–124.
25. Miller TT, Reinus WR. Nerve entrapment syndromes of the elbow, forearm, and wrist. *AJR Am J Roentgenol*. 2010;195:585–594.
26. Jablecki CK, Andary MT, Floeter MK, et al. Practice parameter: electrodiagnostic studies in carpal tunnel syndrome. Report of the American Association of Electrodiagnostic Medicine, American Academy of Neurology, and the American Academy of Physical Medicine and Rehabilitation. *Neurology*. 2002;58:1589–1592.
27. Rempel D, Evanoff B, Amadio PC, et al. Consensus criteria for the classification of carpal tunnel syndrome in epidemiologic studies. *Am J Public Health*. 1998;88:1447–1451.
28. Landis JR, Koch GG. The measurement of observer agreement for categorical data. *Biometrics*. 1977;33:159–174.
29. Isaacs J. Treatment of acute peripheral nerve injuries: current concepts. *J Hand Surg Am*. 2010;35:491–497.
30. Friedrich KM, Chang G, Vieira RL, et al. In vivo 7.0-tesla magnetic resonance imaging of the wrist and hand: technical aspects and applications. *Semin Musculoskelet Radiol*. 2009;13:74–84.
31. Ludwin SK, Maitland M. Long-term remyelination fails to reconstitute normal thickness of central myelin sheaths. *J Neurol Sci*. 1984;64:193–198.
32. Mackinnon SE, Dellon AL, Hudson AR, et al. Chronic human nerve compression—a histological assessment. *Neuropathol Appl Neurobiol*. 1986;12:547–565.
33. Tapadia M, Mozaffar T, Gupta R. Compressive neuropathies of the upper extremity: update on pathophysiology, classification, and electrodiagnostic findings. *J Hand Surg Am*. 2010;35:668–677.
34. Webb S, Munro CA, Midha R, et al. Is multicomponent T2 a good measure of myelin content in peripheral nerve? *Magn Reson Med*. 2003;49:638–645.
35. Does MD, Snyder RE. Multiexponential T2 relaxation in degenerating peripheral nerve. *Magn Reson Med*. 1996;35:207–213.
36. Beaulieu C, Fenrich FR, Allen PS. Multicomponent water proton transverse relaxation and T2-discriminated water diffusion in myelinated and nonmyelinated nerve. *Magn Reson Imaging*. 1998;16:1201–1210.
37. Heule R, Bar P, Mirkes C, et al. Triple-echo steady-state T2 relaxometry of the human brain at high to ultra-high fields. *NMR Biomed*. 2014;27:1037–1045.